INTERNATIONAL JOURNAL FOR NUMERICAL METHODS IN FLUIDS, VOL. 14, 1485–1496 (1992)

A STUDY OF LAMINAR AIR FLOW THROUGH CRACKS BY NUMERICAL SOLUTION OF THE DIFFERENTIAL EQUATIONS

M. R. MOKHTARZADEH-DEHGHAN, A. J. WARD-SMITH AND R. N. WALKER
Department of Mechanical Engineering, Brunel University, Uxbridge, Middlesex UB8 3PH, U.K.

SUMMARY

This paper describes a numerical study of laminar flow through building cracks such as those found around doors or windows. The mathematical model is based on the solution of the two-dimensional conservation equations of mass and momentum by a finite volume method. The results are presented for two crack geometries, namely double-bend and four-bend cracks. The variation in local pressure coefficient along the crack walls and the velocity and pressure distributions within the cracks are described. The overall predicted pressure coefficient for the double-bend crack is compared with the results obtained using a correlation given by Baker *et al.*[5]

KEY WORDS Crack Bend Flow Numerical modelling

1. INTRODUCTION

Building ventilation plays an essential role in the control of the internal environment. Ventilation may be achieved through openings, such as windows, specified during the design stage of the building. It may also result by infiltration through imperfections which include, for example, cracks around doors and windows. The inclusion of the latter type of ventilation is also important in the design of ventilation systems.

The air leakage through building cracks depends on the pressure drop across the crack and the crack geometry. The relationship between the flow rate and pressure drop can be determined by carefully designed experiments.[1,2] A limited number of studies of modelled cracks have been reported which are described below. With the development of computer-modelling techniques, these experimental tests can be simulated with considerably less cost. The present study describes an example of such an approach. It should be noted that although the specific application identified here is building ventilation, flows of this type may be relevant to other types of internal fluid flows, such as those in mitre bends, channels with corrugated walls and seals.

An experimental study of flow through cracks has been reported by Hopkins and Hansford.[3] They considered three crack geometries, namely straight-through, L-shaped and two-bend cracks. They presented their results in the following form, relating the discharge coefficient to the Reynolds number:

$$\frac{1}{c_d^2} = \frac{c_1 z}{Re_h D_h} + c_2, \tag{1}$$

where the Reynolds number is based on the hydraulic diameter D_h, c_1 is a constant, z is the crack

0271–2091/92/121485–12$06.00

Received June 1991
Revised November 1991

length (measured along the centreline; see Figure 1) and c_2 is a loss coefficient associated with the losses at entry, at exit and in bends. For a double-bend crack, Hopkins and Hansford gave values of about 53 and 3·1 for the coefficients c_1 and c_2 respectively. The parameter c_d in equation (1) is defined as

$$c_d = \frac{V}{A}\left(\frac{\rho}{2\Delta p_t}\right)^{1/2}, \tag{2}$$

where V is the volume flow rate, A is the crack area and Δp_t is the overall pressure drop. The term discharge coefficient was first used by Hopkins and Hansford and has the following relationship with a more common term, the pressure coefficient:

$$c_{p_t} = 1/c_d^2. \tag{3}$$

Etheridge[4] re-examined the experimental data of Hopkins and Hansford and suggested new correlations in the same form as equation (1).

More recently, Baker *et al.*[5] reported a detailed experimental study of air flow through cracks of the same basic geometries as those adopted by Hopkins and Hansford. They extended the previous work by considering a wide range of crack heights and lengths and Reynolds numbers. They examined the equations given by Etheridge. Their results showed good agreement with the results of Etheridge as far as the value of c_2 in equation (1) was concerned. However, they obtained somewhat different values for the coefficient c_1. For example, for the double-bend crack the value of c_1 was found to be 78·9 compared with 43·2 given by Etheridge, while the values of c_1 were given as 3·3 and 3·4 respectively. The significant difference between the values of c_2 points to the underestimation of the measured pressure drop across the crack by Hopkins and Hansford.[3] This point will be raised again in Section 6.

This paper describes the results of a numerical study by a finite volume method. For the low flow rates considered here the flow is treated as laminar. Therefore the mathematical model comprises the momentum and continuity equations. Complications associated with the modelling of turbulence, which may occur at higher flow rates, are excluded from the present study.

The contribution of this paper is in the application of computational fluid dynamics to the problem. Also, extension of the work to four-bend cracks (a geometry which has not been considered by the previous authors) provides further insight in the understanding of this type of flow.

2. THE MATHEMATICAL MODEL

It is assumed that the fluid flow through the modelled crack is laminar and two-dimensional. For low flow rates the former assumption is a valid one. The latter assumption is also reasonable since the crack height is relatively small compared with the crack width. Additionally, it is assumed that the flow is steady and incompressible. Thus the governing differential equations describing the conservation of mass and momentum are

$$\frac{\partial u}{\partial x} + \frac{\partial v}{\partial y} = 0, \tag{4}$$

$$u\frac{\partial u}{\partial x} + v\frac{\partial u}{\partial y} = -\frac{1}{\rho}\frac{\partial p}{\partial x} + \nu\left(\frac{\partial^2 u}{\partial x^2} + \frac{\partial^2 u}{\partial y^2}\right), \tag{5}$$

$$u\frac{\partial v}{\partial x} + v\frac{\partial v}{\partial y} = -\frac{1}{\rho}\frac{\partial p}{\partial y} + \nu\left(\frac{\partial^2 v}{\partial x^2} + \frac{\partial^2 v}{\partial y^2}\right). \tag{6}$$

These equations may be solved simultaneously by numerical means. The approach adopted here is an iterative one based on a finite volume method. The discretization of the governing equations into algebraic equations is based on the staggered grid system and hybrid differencing scheme. The solution of the discretized equations incorporates the SIMPLE (semi-implicit method for pressure-linked equations) algorithm[6] for the derivation of pressure, the line-by-line method and tridiagonal matrix algorithm, the under-relaxation procedure and the convergence criterion as described by Ideriah.[7] Additionally, the reader may refer to Reference 8 for further details of the method. The boundary conditions are described in Section 4.

3. CRACK GEOMETRIES

The modelled cracks are the so-called double-bend and four-bend cracks as shown in Figure 1. The geometry of the former is the same as the one defined by Hopkins and Hansford,[3] except for the downstream lengths C_1D_1 and E_1F_1 which are extended for computational purposes (see Section 4). The four-bend crack has been considered here to demonstrate a possible extension of the work to a more complex geometry which may occur in practice. However, experimental data are only available for the double-bend crack.

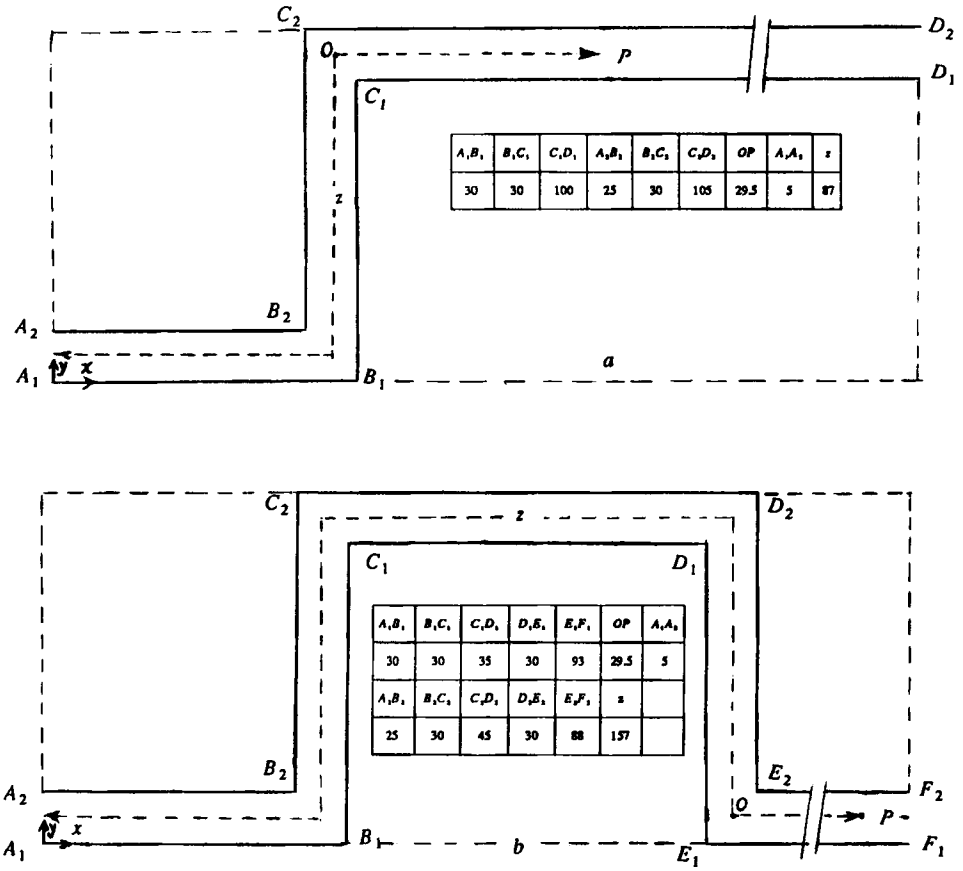

Figure 1. Crack geometrics: (a) double-bend crack; (b) four-bend crack (dimensions are in millimetres)

4. COMPUTATIONAL DETAILS

The Cartesian co-ordinate system (x–y) is shown in Figure 1. It was applied without change over the entire flow field.

The results are presented for grid sizes 34×34 and 58×34 for double-bend and four-bend cracks respectively. The distribution of grid lines may be realized with reference to the vector plots of the velocity fields shown in Figures 2 and 3. Two other grid sizes, namely 70×42 and 46×26 for the four-bend and 38×42 and 30×26 for the two-bend crack, were also considered. The coarser grid sizes did not provide accurate representations of the flow fields, since the recirculation zones at the corners were not predicted or their sizes were underestimated. The finest grids, on the other hand, did not result in significantly different results from those obtained using 34×34 and 58×34 grids.

The hydraulic diameter is defined as

$$D_h = 4A/P, \tag{7}$$

where A and P are the cross-sectional area and the wetted perimeter respectively. When the crack height is much smaller than its width, equation (7) reduces to

$$D_h = 2h. \tag{8}$$

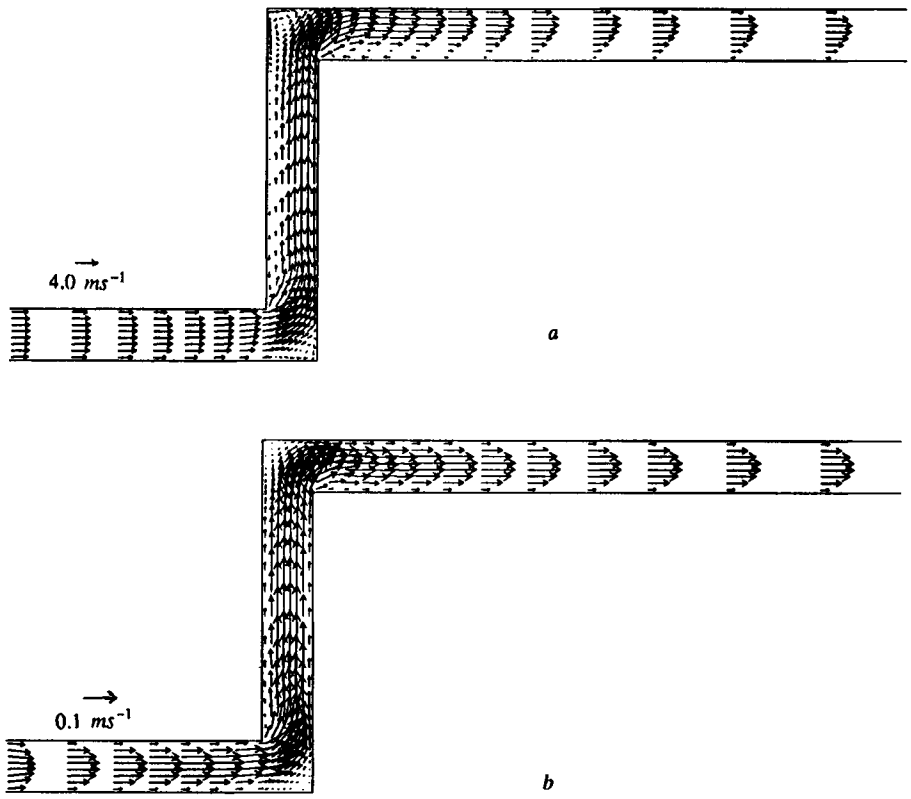

Figure 2. Vector plots of the velocity field in a double-bend crack: (a) $Re_h = 2000$; (b) $Re_h = 50$

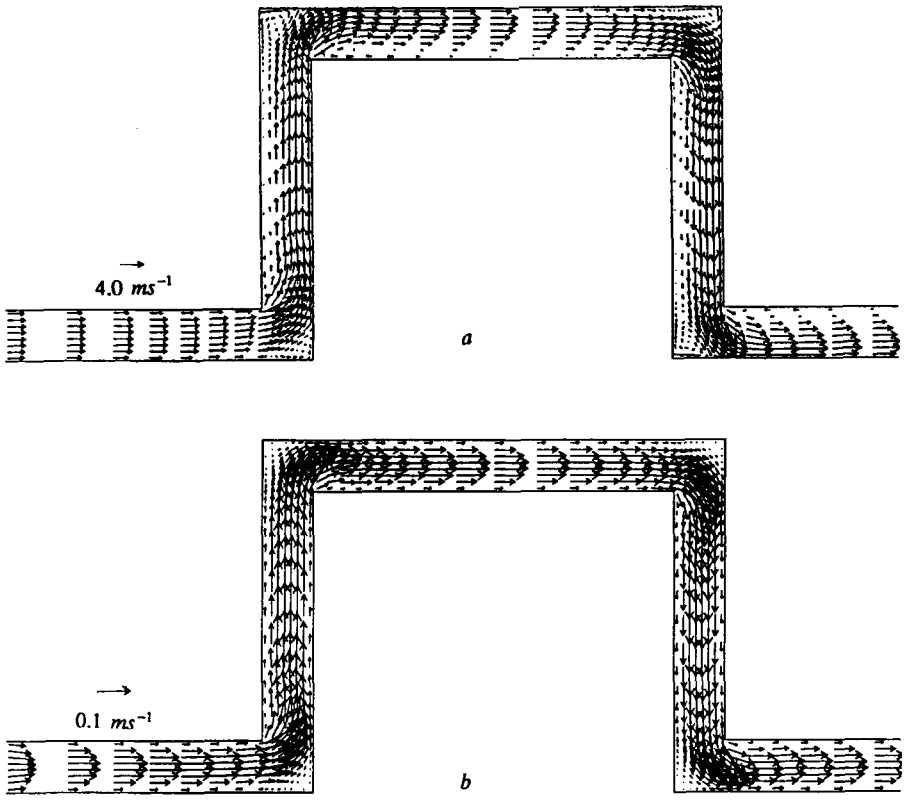

Figure 3. Vector plots of the velocity field in a four-bend crack: (a) $Re_h = 2000$; (b) $Re_h = 50$

The Reynolds number is defined as

$$Re_h = D_h U/\nu, \tag{9}$$

where U is the average velocity. This definition, based on D_h rather than h, was chosen so that the results are directly comparable with those of Baker *et al.*[5]

The local pressure p is computed relative to the pressure at the crack inlet.

The local pressure drop Δp_l is defined as the difference between the local pressure and the pressure at the inlet and therefore has the same numerical value as the local pressure. The overall pressure drop Δp_t, is measured at a location downstream of the last bend, indicated by P in Figure 1. The location of P was chosen so that the overall crack length z was the same as the one adopted by Hopkins and Hansford.[3]

The local pressure coefficient is defined as

$$c_{p_l} = \Delta p_l / \tfrac{1}{2}\rho U^2. \tag{10}$$

The overall pressure coefficient is defined similarly but with Δp_t in the numerator.

The boundary conditions were defined as follows.

At the crack inlet a uniform velocity was assumed. The Reynolds number was in the range 50–2000, which corresponds to an average velocity in the range 0·076–3·0 $m s^{-1}$. The air properties were calculated at 20 °C.

At the outlet the flow was assumed to be parallel (in the main flow direction) and the v-component of velocity was set to zero. The value of the u-component was adjusted so that the total inflow and the total outflow mass flow rates remained the same. In order to satisfy this boundary condition at the outlet, the length of the crack downstream of the last bend was extended (see Figure 1). However, the calculation of the overall pressure drop was based on the value of the pressure at a location well before the outlet, as was mentioned in Section 3.

At the walls the non-slip condition was applied and the wall shear force on the flow was introduced via the source terms in the discretized momentum equations. The areas shown by the broken lines in Figure 1 were treated as solid regions.

The computer program used in this study has been applied to and tested on numerous problems (see e.g. References 9 and 10).

5. RESULTS

Two examples of the velocity field for the double-bend and four-bend cracks (for $Re_h = 2000$ and 50) are shown in Figures 2 and 3. Contour plots of the pressure field for the four-bend crack are shown in Figure 4. The variation in local pressure coefficient along the upper and lower walls is shown in Figures 5 and 6. Finally, a comparison between the predicted results and the

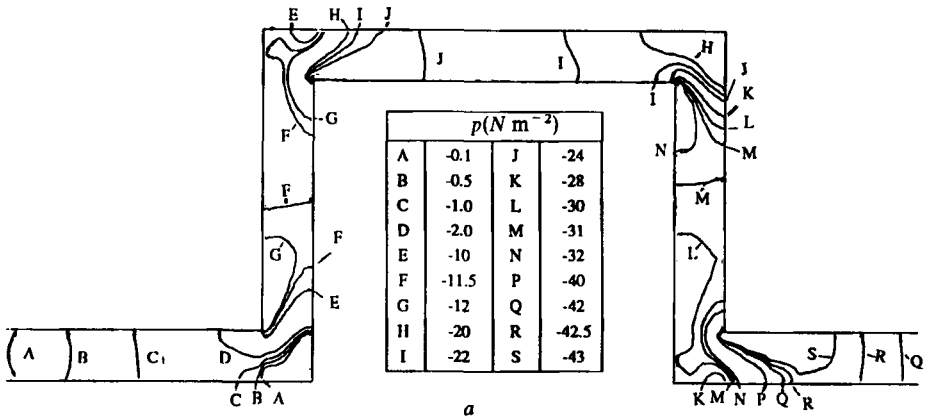

Figure 4. Contour plots of the pressure in a four-bend crack: (a) $Re_h = 2000$; (b) $Re_h = 50$

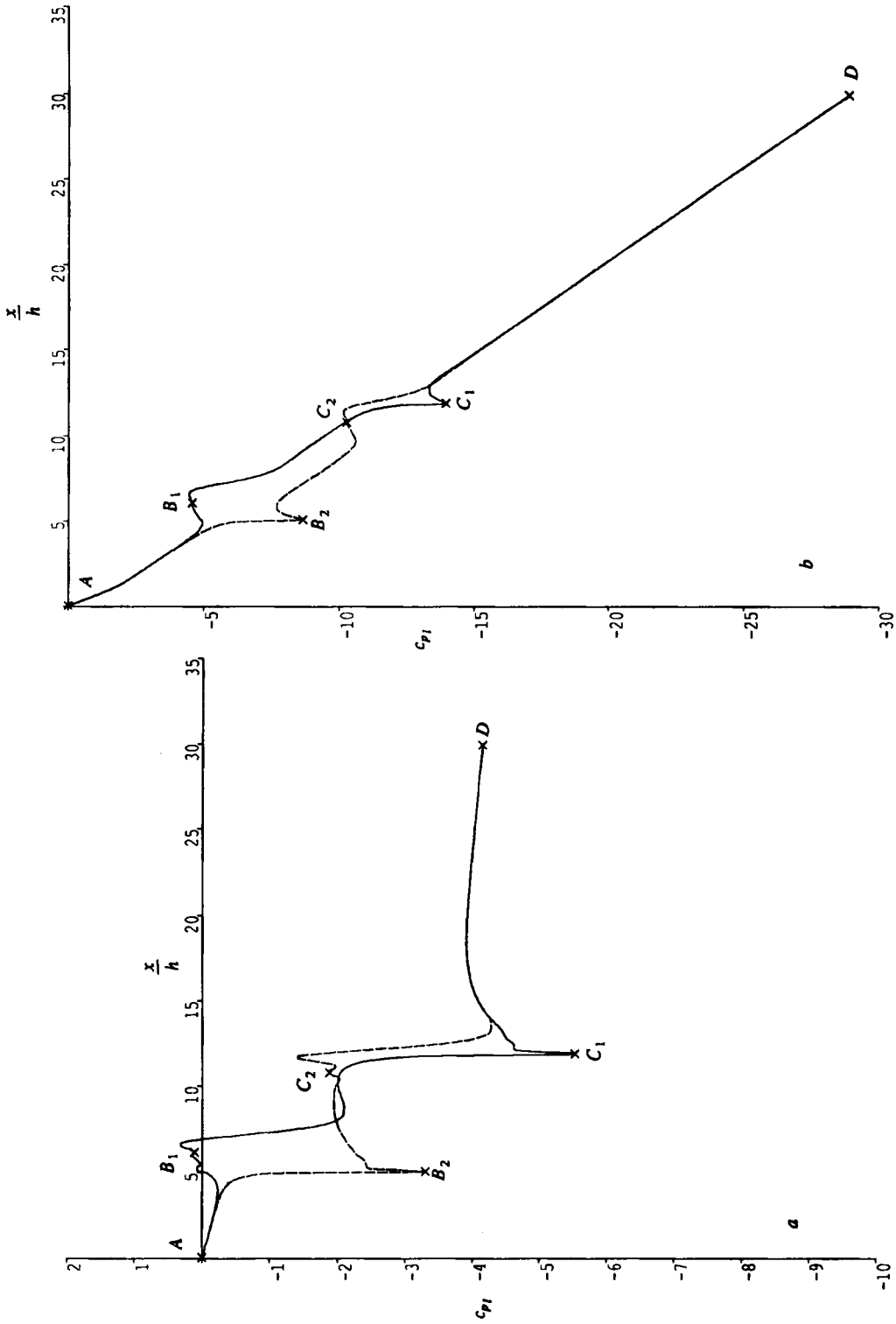

Figure 5. Variation in pressure coefficient along the lower and upper walls of a double-bend crack: (a) $Re_h = 2000$; (b) $Re_h = 50$

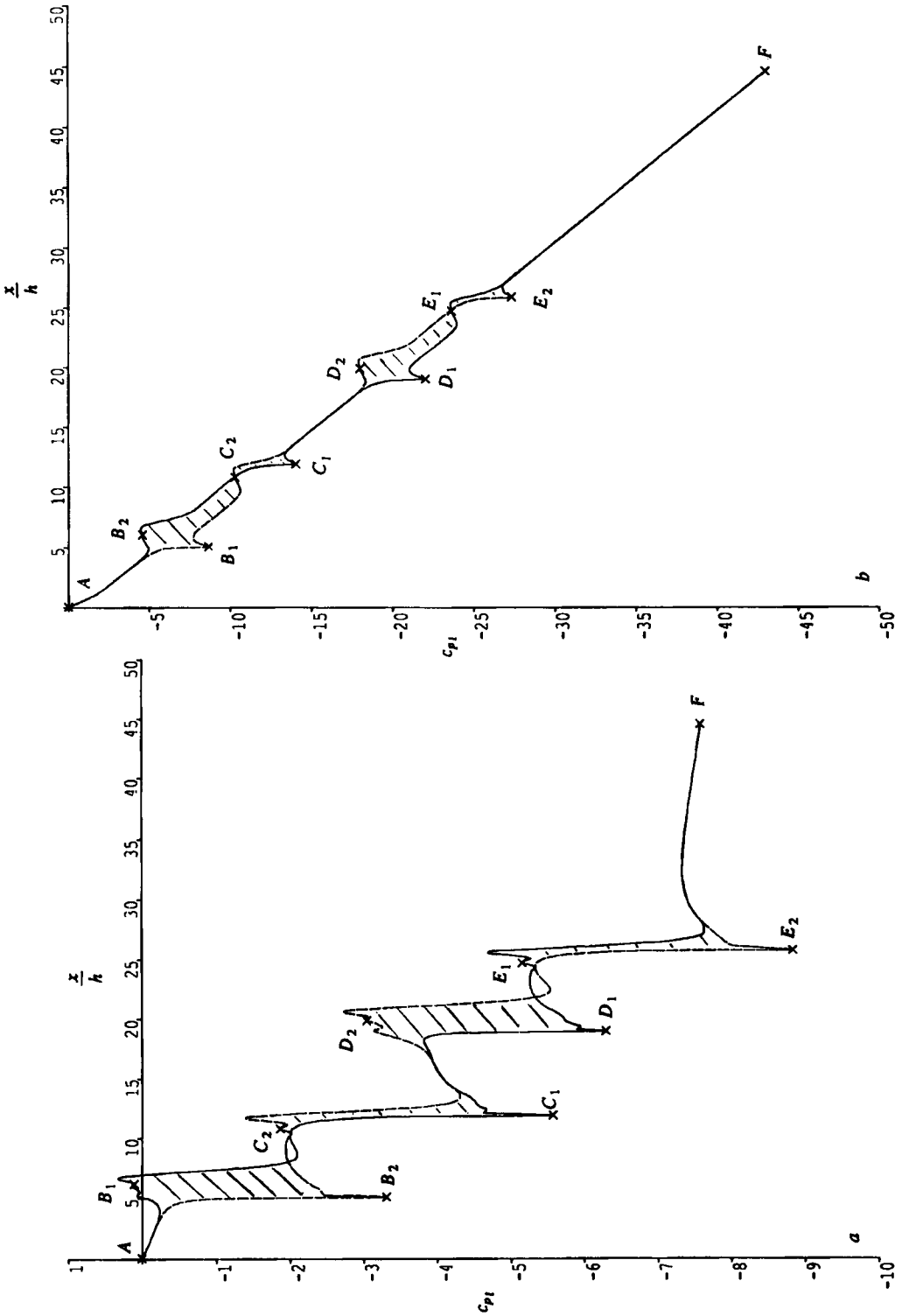

Figure 6. Variation in pressure coefficient along the lower and upper walls of a four-bend crack: (a) $Re_h = 2000$; (b) $Re_h = 50$

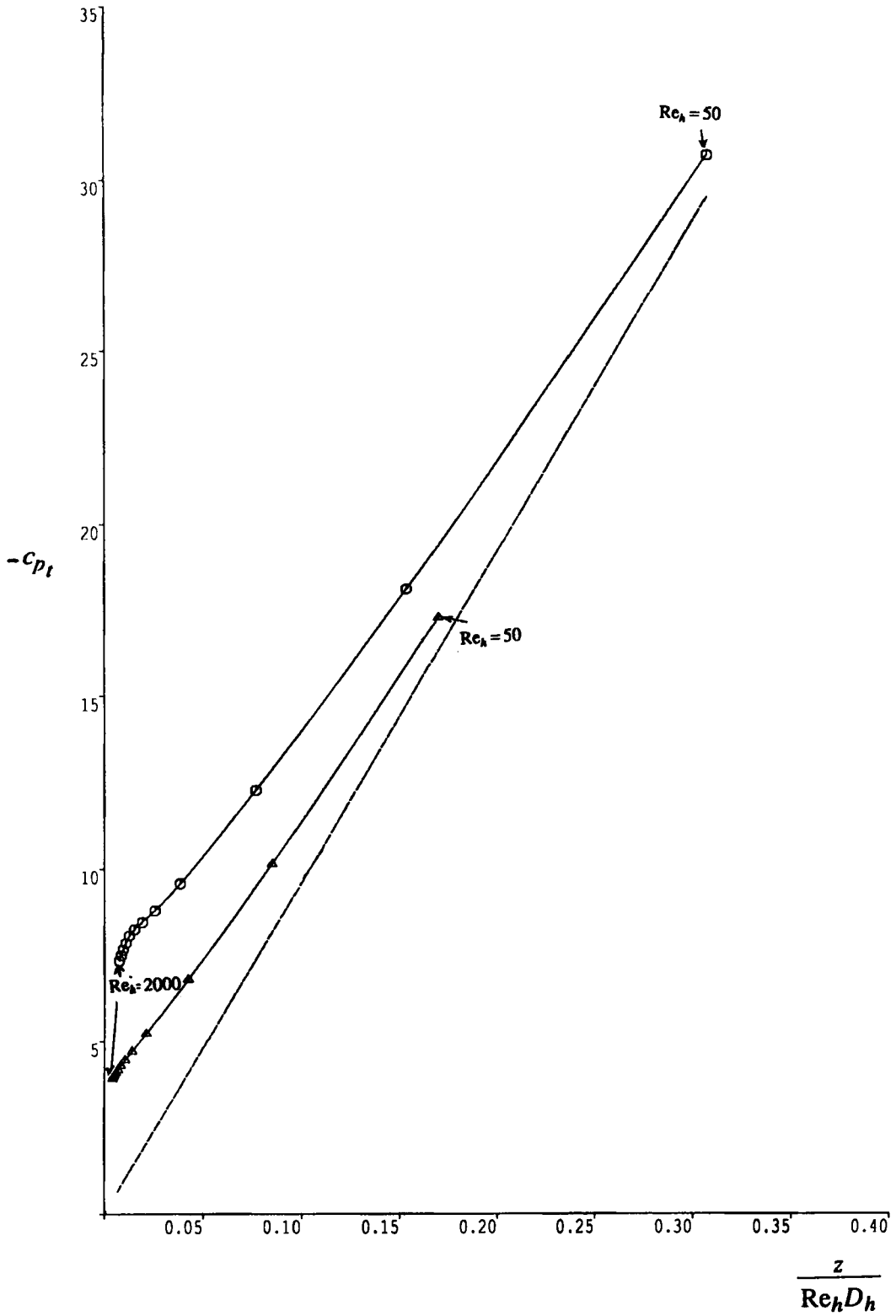

Figure 7. Variation in overall pressure coefficient: △, double-bend crack; ○, four-bend crack; ----, laminar flow between two parallel plates (see equation (12))

experimental data for the double-bend crack is shown in Figure 7. This figure also shows the results for the four-bend crack. The results for a fully developed laminar flow between two parallel plates are also included for comparison.

6. DISCUSSION

The velocity field for the four-bend crack and $Re_h = 2000$ (see Figure 3(a)) shows flow separation at the sharp corners (B_2, C_1, D_1 and E_2 in Figure 1) on the inner wall and subsequent reattachment and thus formation of recirculation zones. These recirculation zones are absent for $Re_h = 50$ (see Figure 3(b)). However, results not shown here indicated that recirculation zones were present for Reynolds numbers as low as 100 and that their sizes decreased with decreasing Reynolds number. There are also recirculation zones at the corners (B_1, C_2, D_2 and E_1) on the outer walls. The sizes of these regions, however, remained nearly independent of the Reynolds number. The flow field for a Reynolds number of 50 shows a tendency to establish a parabolic velocity profile within each leg of the bend.

Comparing the velocity fields for the double-bend and four-bend cracks (Figures 2 and 3) indicates that the flow patterns are virtually the same within the first two legs (AB and BC) of the bends and that the downstream bends have no or little effect on the upstream flow. This was also confirmed by comparing the contour plots of the pressure fields shown in Figure 4 with those for the double-bend crack (not shown here). These figures indicate a large variation in pressure around the corners. The pressure is, however, nearly constant across the crack in the middle region of each leg away from the corners.

The variation in local pressure coefficient along the walls (see Figures 5 and 6) demonstrates the familiar behaviour observed in bends,[10-12] i.e. the adverse and then favourable pressure gradients on the outer wall and vice versa on the inner wall of each bend. An interesting feature of these multi-bends is that as the flow direction is followed, the inner wall (or outer wall) of one bend will become the outer wall (or inner wall) of the following bend. This is reflected in the type of pressure variation seen here, which is specific to this type of bend. Along a significant part of the crack length, between C_1 and D_1, the pressure on both walls remains the same. This behaviour is absent between, say, B_1 and C_1. It is interesting to note the alternate formations of wide and narrow regions of pressure variation indicated by the shaded areas in Figure 6. The reason for this behaviour can be realized with reference to Figures 2 and 5. The flow, in going from B_2 towards C_2 (the inner wall of the first bend followed by the outer wall of the second bend), experiences an adverse pressure gradient in the neighbourhood of the second bend. The opposite is the case for the flow along B_1C_1, where it experiences mostly a favourable pressure gradient along its path. This phenomenon is also manifested in the formation of different (in size and extent) recirculation zones on B_2C_2 (and D_1E_1) compared with C_1D_1 (and E_2F_2).

Figure 7 shows the effect of the Reynolds number on the overall pressure coefficient. As the Reynolds number increases, the pressure coefficient decreases. For the same Reynolds number the four-bend crack shows, as expected, a higher pressure coefficient than the two-bend crack. However, it should be noted that since the length z is different for the two-bend crack than the four-bend crack, a particular value of z/Re_hD_h corresponds to different Reynolds numbers for the two different types of cracks.

On the basis of their experimental work, Baker *et al.*[5] suggested the following correlation for a double-bend crack:

$$c_{p_t} = 78{\cdot}9\,\frac{z}{D_h Re_h} + c_2. \tag{11}$$

The present numerical calculations are of approximately the same mathematical form as equation (11). However, the curvature of the lines representing both the double-bend and four-bend configurations indicates that the coefficient c_2 is a (weak) function of the Reynolds number. This is not entirely surprising, since it is equivalent to stating that the pressure losses associated with the bends are (weak) functions of the Reynolds number.

The value of c_2 specified by Baker *et al.*[5] was 3·3. However, this value includes effects associated with flow contraction into and expansion from the cracks. A consistent basis of comparison of the experimental work of Baker *et al.* with the present numerical work can be obtained by adjusting their value for c_2 by subtracting an appropriate amount for the combined effects of entry and exit losses. Baker *et al.* estimated that these two components made a contribution of 1·5 to their value of c_2. Hence for comparison with the present work the appropriate value of c_2 is $3{\cdot}3-1{\cdot}5=1{\cdot}8$.

With this value of c_2 the predicted results are about 12% higher than those obtained from equation (11). However, the disagreement is not as severe as it might appear. The experimental data of Baker *et al.*[5] show about the same percentage deviation from the mean value. In their error analysis they estimated errors of about 2% in the value of $z/Re_h D_h$ and 3% in c_{p_t} for 6 mm cracks. For thinner cracks they estimated higher values. However, their analysis was based on errors associated with the crack height and no analysis of the errors associated with the pressure and volume flow measurements were presented.

Comparison with the results obtained using the theory of laminar flow between two parallel plates may be useful in this respect. This theory (for a fully developed velocity profile) yields

$$c_{p_t}=96\frac{z}{D_h Re_h}. \tag{12}$$

This relationship is also shown in Figure 7. As expected, the pressure coefficient evaluated using equation (12) is lower than the values obtained experimentally for cracks (for the obvious reason that the presence of bends causes additional losses), but only up to a value of about $z/D_h Re_h=0{\cdot}1$. For larger values the experimental correlation actually shows lower pressure drops. High values of $z/D_h Re_h$ correspond to low values of Re_h and hence low flow rates and differential pressures. For example, a Reynolds number of about 50 corresponds to an average velocity of about $0{\cdot}076\ \mathrm{m\,s^{-1}}$ and a flow rate (per unit width) of about $37{\cdot}5\times10^{-5}\ \mathrm{m^2\,s^{-1}}$. It is particularly difficult to obtain accurate measurements under these demanding conditions, and experimental results frequently show greater error under such circumstances. Since there is no significant reduction in the present computational accuracy at high values of $z/D_h Re_h$, it must be inferred that the noted discrepancy is attributable to experimental errors. Comparing the present numerical results with those based on equation (12), however, shows that higher pressure drops are predicted over the entire range of $z/Re_h D_h$ shown in Figure 7.

It may also be useful to refer to the correlation by Etheridge[4] at this stage. On the basis of results of Hopkins and Hansford,[3] a value of 43·2 was suggested for c_1 compared with 78·9 as suggested by Baker *et al.*[5] This obviously results in significant underestimation of the pressure coefficient, much lower than what equation (11) yields.

7. CONCLUSIONS

A numerical study of laminar fluid flow through building cracks was presented. The results showed details of the flow field, such as regions of flow separation and local pressure distributions. These details are very difficult to obtain by experimental means.

The predicted overall pressure coefficient for a double-bend crack was higher than that obtained using the correlation by Baker *et al.*[5] It is argued that the discrepancy is explained by the

experimental correlation underestimating the pressure coefficient, especially at very low flow rates.

The results show that computational fluid dynamics can be used as an effective tool in increasing understanding of complex flows and in obtaining data on gross parameters (the overall pressure drop in this case), especially in areas where accurate measurements are difficult to obtain.

APPENDIX: NOMENCLATURE

A	area
c_1, c_2	constants in equation (1)
c_d	discharge coefficient
c_{p_l}	local pressure coefficient (see equation (10))
c_{p_t}	overall pressure coefficient
D_h	hydraulic diameter (see equation (8))
h	crack height
p	pressure
P	perimeter
Re_h	Reynolds number based on the hydraulic diameter
u, v	components of velocity in x- and y-direction respectively
U	average velocity
V	volume flow rate
x, y	Cartesian co-ordinate system
z	crack length
Δp_t	overall pressure drop
Δp_l	local pressure drop
ρ	density
ν	kinematic viscosity

REFERENCES

1. P. T. McGrath and A. T. Howarth, 'Measurements of air flows through cracks between building components', *Build. Serv. Eng. Res. Technol.*, **5**, 43–48 (1984).
2. C. Y. Shaw, 'Methods for conducting small-scale pressurisation tests and air leakage data of multi-storey apartment buildings', *ASHRAE Trans.*, **86**, pt. 1, 241 (1980).
3. L. P. Hopkins and B. Hansford, 'Air flow through cracks', *Build. Serv. Eng.*, **42**, 123–129 (1974).
4. D. W. Etheridge, 'Crack equations and scale effects', *Build. Environ.*, **12**, 181–189 (1977).
5. P. H. Baker, S. Sharples and I. C. Ward, 'Air flow through cracks', *Build. Environ.*, **22**, 293–304 (1987).
6. S. V. Patankar and D. B. Spalding, 'Turbulence models and their application to the prediction of internal flows', *Heat Fluid Flow*, **2**, 43–54 (1972).
7. F. J. K. Ideriah, 'Prediction of turbulent cavity flow driven by buoyancy and shear', *J. Mech. Eng. Sci.*, **22**, 287–295 (1980).
8. S. V. Patankar, *Numerical Heat Transfer and Fluid Flow*, McGraw Hill, New York, 1980.
9. M. M. M. El Telbany, M. R. Mokhtarzadeh-Dehghan and A. J. Reynolds, 'Single sided ventilation—Part I. The flow between a cavity and external air stream', *Build. Environ.*, **20**, 15–24 (1985).
10. N. A. E. Kotb, M. R. Mokhtarzadeh-Dehghan and A. J. Ward-Smith, 'A numerical study of laminar and turbulent flows in a two-dimensional bend with or without a guide vane', *Int. j. numer. methods eng.*, **26**, 245–262 (1988).
11. A. J. Ward-Smith, *Pressure Losses in Ducted Flows*, Butterworths, London, 1971.
12. A. J. Ward-Smith, *Internal Fluid Flow*, Oxford University Press, Oxford, 1980.